RESEARCH ARTICLE
doi: 10.2306/scienceasia1513-1874.2025.024

ScienceAsia 51 (2): 2025: ID 2025024: **1–11**

Catalytic influence on biomass gasification behaviour in nickel-modified natural zeolite catalysts

Imron Rosyadi[a], **Suyitno**[a,*], **Zainal Arifin**[a], **Tata Sutardi**[b], **Andika Taufiqurohman**[c], **Muji Setiyo**[d], **Wibawa Endra Juwana**[a]

[a] Department of Mechanical Engineering, Faculty of Engineering, Universitas Sebelas Maret (UNS), Indonesia
[b] Research Centre for Energy Conversion and Conservation, BRIN, Indonesia
[c] Department of Mechanical Engineering, Faculty of Engineering, Universitas Sultan Ageng Tirtayasa, Indonesia
[d] Department of Mechanical Engineering, Faculty of Engineering, Universitas Muhammadiyah Magelang, Indonesia

*Corresponding author, e-mail: suyitno@staff.uns.ac.id

Received 7 Mar 2024, Accepted 25 Feb 2025
Available online 22 Apr 2025

ABSTRACT: This study rigorously investigates biomass thermal behavior and gasification efficiency using natural zeolite (NZ) catalysts, specifically focusing on those modified with nickel. Objectives encompass the assessment of Si/Al ratio, surface area, and pore characteristics of zeolite catalysts. Thermogravimetric Analysis exposes distinct temperature-dependent biomass behaviors, emphasizing nickel's catalytic influence, notably in Ni/NZMC at 471.95 °C, indicating enhanced thermal interactions linked to cellulose decomposition. Structural changes due to nickel impregnation are detailed through X-ray diffraction patterns, revealing shifts in peak heights and Si/Al ratios. The syngas composition analysis highlights Ni/NZMC's exceptional hydrogen production. Gasification yield results underscore zeolite catalysts' positive impact, particularly Ni/NZMC, exhibiting superior efficiency with increased gas yield and higher hydrogen content. This research challenges conventional beliefs, unveiling a nuanced relationship between Si/Al ratio, specific surface area, and gasification results, emphasizing the multifaceted nature of catalyst performance. These findings significantly contribute to understanding catalyst-driven biomass conversion, providing a strong foundation for sustainable energy advancements.

KEYWORDS: catalyst, natural zeolite, nickel impregnation, biomass gasification, syngas production, renewable energy

INTRODUCTION

The remarkable properties of natural zeolites have propelled their widespread applications across diverse fields, attracting considerable attention from researchers and industries alike [1–3]. Characterized by well-defined porous structures and ion-exchange capabilities, natural zeolites exhibit versatility in applications ranging from agronomy, ecology, and manufacturing to medicine, cosmetics, and various catalytic processes, including the pivotal roles in pyrolysis and transesterification of palm oil [4, 5]. However, the effectiveness of natural zeolites is intricately linked to specific applications and the inherent properties of the zeolites used, presenting challenges such as pore size effects, acidity changes, and stability concerns that underscore the need for meticulous consideration in their utilization [1, 6–9].

In the pursuit of sustainable energy production, biomass gasification has emerged as a promising technology, offering a pathway to renewable and carbon-neutral energy sources [9, 10]. Central to the success of biomass gasification is the use of natural zeolites as catalysts, addressing challenges like the formation of undesirable tar byproducts [11–13]. Through modification, natural zeolites become effective catalysts for tar cracking, enhancing cold gas efficiency and increasing the hydrogen and carbon monoxide content in the resulting product gas [15]. Optimization of the pore structure, achieved through pre-treatment processes like dealumination and desilication, is essential to mitigate mass diffusion issues and prevent the formation of undesirable byproducts during gasification processes.

The modification of natural zeolites not only enhances catalytic activity but also plays a crucial role in ensuring the stability of the catalyst during prolonged and challenging conditions of biomass gasification. The crucial role of stability in nickel-impregnated natural zeolites for extended activity, particularly in diverse catalytic reactions such as hydro conversion and green diesel production, was highlighted. The modification of Indonesian natural zeolite (NZ) with varying nickel content (3%, 5%, and 10 wt.%) revealed that the 3% Ni-modified NZ exhibited superior activity (77.34%) and selectivity (53.11%) on C15 in catalytic tests at 375 °C and 12 bar pressure for 2 h, emphasizing the effectiveness of nickel modification, especially in the realm of green diesel production from crude palm oil (CPO) [16]. Nickel (Ni) is a transition metal with great potential for various applications, especially in semiconductor rectifiers, gas sensors, and high-performance catalysts. Among transition metals such as Ni, Fe, Co, Mn, Cu, and Zn, nickel has the best catalytic ability and is superior to iron (Fe) [17].

Although nickel-impregnated zeolite catalysts exhibit advantages in various applications, they come with potential drawbacks. Firstly, there is a risk of coke formation, a phenomenon that can deactivate the catalyst over time, particularly concerning when the catalyst has a high density of Brønsted acid sites [16–18]. Additionally, the pore size of the zeolite plays a role in the catalyst's performance; for instance, zeolites with narrower pores, like Y type zeolite supported nickel catalysts, can encourage coke deactivation [19–22]. Nickel impregnation alters zeolite acidity, influencing catalytic activity, and introducing changes in properties, as seen in Ni-modified ZSM-5 zeolites, which exhibit enhanced stability and isomerization selectivity due to a synergistic effect between Brønsted and Lewis acid sites [23–26]. Finally, the stability of nickel-impregnated zeolites, influenced by factors like the nickel impregnation method, concentration, and zeolite properties, is explored in multiple studies, demonstrating enhanced stability and isomerization selectivity in impregnated ZSM-5 zeolites compared to in situ synthesis, with nickel contents ranging from 3% to 10% in studies focusing on green diesel production and carboxylation reactions [16, 25], excluding biomass gasification. Nevertheless, further research is needed to determine the effectiveness of Ni-impregnated NZ in biomass gasification applications. These catalysts present potential challenges, including issues related to coke formation, pore size effects, and changes in acidity, necessitating careful consideration when applied in biomass gasification.

The principal objectives of this study are to systematically investigate the thermal behavior and gasification efficiency of biomass in the presence of diverse NZ catalysts, with a particular emphasis on those subject to modification and nickel impregnation. The study seeks to unravel the intricate interplay among catalyst characteristics, temperature-dependent behaviors, and biomass composition during thermal degradation. Furthermore, the research aims to comprehensively characterize the structural and compositional alterations in zeolite catalysts induced by modification and nickel impregnation, offering crucial insights into the catalyst's pivotal role in biomass conversion processes. The specific objectives encompass the quantitative assessment of the Si/Al ratio, surface area, and pore characteristics of the zeolite catalysts. Additionally, the study aims to conduct a detailed analysis of the temperature-dependent behaviors of biomass utilizing Thermogravimetric Analysis (TGA). Furthermore, the investigation will evaluate the syngas composition and gasification efficiency across various catalyst conditions. By achieving these objectives, the study aspires to make significant contributions to the understanding of catalytic biomass conversion, fostering advancements in sustainable energy production within the scientific community and industry.

MATERIALS AND METHODS

Materials used

The gasification process relied on a combination of Municipal Solid Waste (MSW) sourced from TPSA Cilowong, Serang, Banten Province, Indonesia, and coconut shell biomass from a traditional market. The MSW mixture contains 49.07% carbon, 6.05% hydrogen, 39.79% oxygen, and 0.95% nitrogen, while the coconut shell biomass has a composition of 47.63% carbon, 6.29% hydrogen, 45.42% oxygen, and 0.13% nitrogen. To prepare these materials, they were first dried at 105 °C for 3 h to reduce the moisture content. The coconut shell biomass obtained from a traditional market was blended in a 60:40 mixing ratio.

In catalyst synthesis, natural zeolite served as the foundational material, chosen for its porosity and ion-exchange capabilities essential for catalytic applications. Modified natural zeolites, specifically NZMA, NZMB, NZMC, NZMD as well as Ni/NZMA, Ni/NZMB, and Ni/NZMC, Ni/NZMD were produced in the process. Nickel nitrate ($\mathrm{Ni(NO_3)_2 \cdot 6\,H_2O}$) was selected as the nickel precursor for impregnation due to its solubility and effective release of nickel ions. The concentration of nickel nitrate was carefully controlled to influence the final nickel content in the catalyst.

During impregnation, solvents were utilized based on their compatibility with the catalyst and nickel nitrate. The choice of solvent, whether water or organic solvents, was made to ensure the uniform dispersion of nickel nitrate on the modified zeolite surface. In the BET analysis, nitrogen gas was employed to evaluate the surface area and porosity of the catalyst. The controlled adsorption of nitrogen at low temperatures provided essential data for understanding the physical characteristics of the modified natural zeolites impregnated with nickel (Ni/NZMA, Ni/NZMB, Ni/NZMC, and Ni/NZMD), collectively referred to as the Ni-NZM catalyst.

Synthesis of NZM and Ni-NZM catalyst

In the initial phase, natural zeolite underwent modification to enhance its surface area and Si/Al ratio. A carefully selected natural zeolite was subjected to a modification process aimed at increasing its porosity and altering its chemical composition. This process involved treatments such as dealumination and desilication, optimizing the pore structure to address potential mass diffusion issues during subsequent catalytic reactions.

Initially, raw NZ, sourced from Bayah, Banten, Indonesia, undergoes physical examination, sorting, and grinding. The resulting fine powder is sieved to achieve a mesh size of 80 for uniformity. Subsequently, the zeolite powder is dried by baking in an oven at 300 °C for 30 min, followed by activation through immersion in a 4% hydrofluoric acid (HF) solution at a ratio of 1:2 (w/v) for 30 min, and subsequent washing with water.

For NZMA, the activated zeolite undergoes refluxing in 6 M HCl for 30 min at 90 °C. NZMB involves an additional step of soaking the zeolite for 24 h after refluxing. NZMC undergoes an extended reflux process for 120 min. NZMD involves reflux process for 120 min and an additional step of soaking the zeolite for 24 h. The products from the reflux process are washed with water until the wastewater reaches a pH of 5, and then dried at 120 °C. Ion exchange is carried out by immersing the zeolite in a 0.1 M ammonium chloride (NH_4Cl) solution at a ratio of 1:2 (v/v) for 3 h at 90 °C. This process involves the exchange of cations such as K, Fe, and Ca with NH_4^+, enhancing the overall acidity of the zeolite. The final step is calcination, where the zeolite is heated at 600 °C for 4 h, leading to the decomposition of NH_4^+ ions into H^+ ions and forming H-zeolite. The variations in the synthesis steps result in the formation of NZMA, NZMB, and NZMC, each possessing distinct properties and characteristics.

After the modification of natural zeolite into NZMA, NZMB, NZMC, and NZMD, the catalyst precursor was prepared by impregnating the modified zeolite with nickel nitrate ($Ni(NO_3)_2 \cdot 6\,H_2O$). The impregnation process played a crucial role in introducing nickel species onto the zeolite surface, enhancing its catalytic properties. The concentration of nickel nitrate was meticulously controlled to achieve the desired nickel content in the final catalyst. The impregnated zeolite was then left to stand, ensuring the proper penetration of the nickel precursor. Following impregnation, the zeolite underwent a drying process to eliminate any residual solvent or water. This step was essential to prepare the catalyst precursor for the subsequent calcination process. The drying occurred at a controlled temperature of 120 °C, facilitating the removal of moisture without inducing undesired chemical changes. The dried catalyst precursor then underwent calcination to transform into the final Ni-NZM catalyst. Calcination was conducted at an elevated temperature of 800 °C for a specified duration of 3 h. The synthesis of NZM and Ni-NZM catalysts are clarified on a schematic diagram of the activation of the zeolite process for Ni-zeolite impregnation and its characterization (Fig. 1). This thermal treatment served to remove any remaining organic components, activate the nickel species, and stabilize the modified zeolite structure. The resulting Ni-NZM catalyst was then ready for further analysis and testing.

Characterization techniques

The Brunauer-Emmett-Teller (BET) analysis was employed to evaluate the surface area and porosity of the Ni-NZM catalyst. Nitrogen adsorption at low temperatures was applied to the catalyst, and the resulting isotherm was utilized to ascertain specific surface area, pore volume, and pore size distribution.

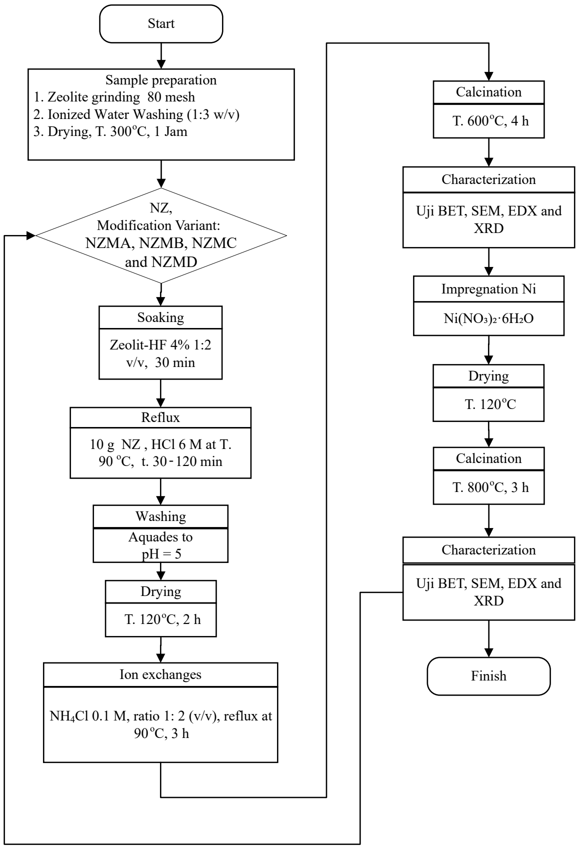

Fig. 1 The schematic diagram of the activation zeolite process to Ni-zeolite impregnation and its characterization.

BET analysis yielded insights into the physical properties of the catalyst, which were crucial for comprehending its performance in subsequent catalytic processes. Scanning Electron Microscopy (SEM) was utilized to visualize the morphology and structure of the Ni-NZM catalyst in the past. This high-resolution imaging technique facilitated the examination of surface features, particle size distribution, and the overall microstructure of the catalyst. The analysis via SEM provided valuable information on the physical characteristics of the catalyst, contributing to the assessment of its suitability for biomass gasification. Energy-Dispersive X-ray Spectroscopy (EDS) was applied in the past to determine the elemental composition of the Ni-NZM catalyst, with a specific emphasis on evaluating the distribution of nickel within the zeolite matrix. EDS analysis generated quantitative data on the nickel content, confirming the successful impregnation of nickel species onto the zeolite surface.

Gasification tests and syngas composition analysis

The Ni-NZM catalyst underwent gasification tests in a fixed bed gasifier to assess its performance in biomass gasification (Fig. 2). Gasification conditions, involv-

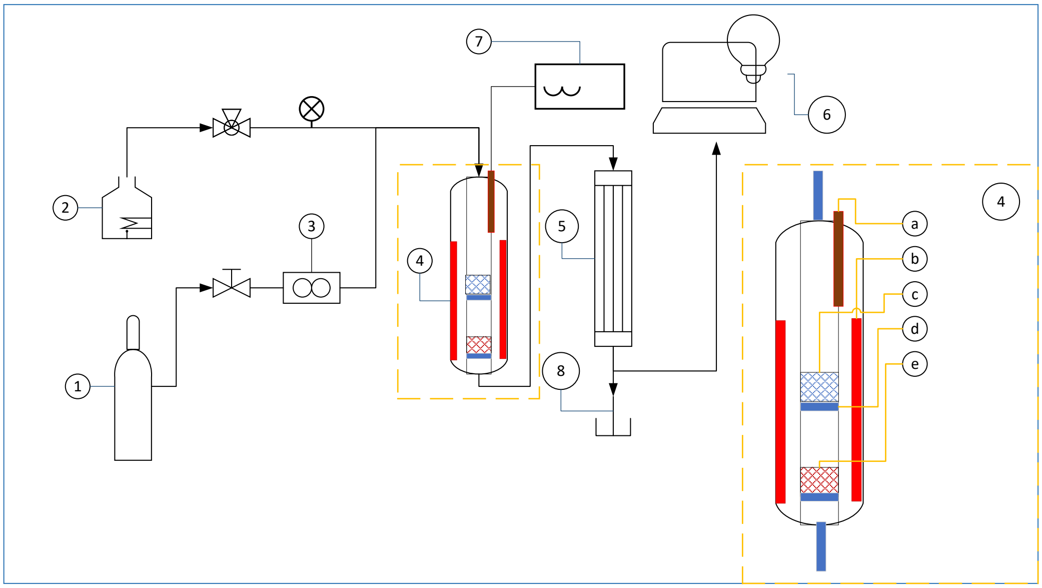

Fig. 2 An updraft fixed bed gasification reactor, consisting of the following components: (1) Nitrogen Gas Inlet, (2) Steam Generator, (3) Mass Flow Meter, (4) Gasifier Reactor with subcomponents: a. Thermocouple, b. Heater Element, c. Catalyst, d. Perforated Plate, e. Biomass, (5) Condenser Unit, and (6) Gas Analysis, (7) Temperature Controller.

ing temperature and pressure, were meticulously controlled to replicate real-world operating conditions. The catalyst's capacity to generate syngas from biomass feedstock was evaluated, with a specific focus on the production of hydrogen-rich syngas. To augment the production of hydrogen-rich syngas, steam was introduced into the reactor at a ratio of 1:3 steam to biomass.

Gas Chromatography-Mass Spectrometry (GCMS) was utilized for the analysis of the syngas composition. The generated syngas was sampled, and the GCMS system was employed to separate and quantify individual components, including hydrogen, carbon monoxide, methane, and other trace gases. This analysis provided detailed insights into the catalytic performance of Ni-NZM, particularly concerning the production of hydrogen-rich syngas.

The outlined methodology ensured a systematic and thorough approach to the synthesis, characterization, and testing of the Ni-NZM catalyst, contributing to a comprehensive understanding of its potential in biomass gasification applications.

RESULTS AND DISCUSSION

Properties of raw and modified NZs

Table 1 serves as a comprehensive overview, shedding light on critical characteristics of both raw and modified natural zeolite (NZ) catalysts, as well as their Ni-loaded derivatives (Ni/NZA, Ni/NZB, Ni/NZC and Ni/NZD). A crucial factor influencing catalytic performance, the Si/Al ratio, is prominently displayed. The modified NZ samples (NZA, NZB, NZC, NZD) show a significant increase in Si/Al ratio, especially noteworthy in NZD with a value of 27.05. This suggests a successful modification process, potentially enhancing the catalyst's catalytic activity [29]. Concurrently, the surface area, a key determinant of catalytic efficiency, experiences a substantial increase in the modified catalysts compared to the raw NZ, with NZA exhibiting the highest surface area at 147.7 m^2/g, followed closely by NZB at 136.3 m^2/g. This augmentation can be attributed to the modification process, indicating a higher availability of active sites for catalytic reactions [29]. The higher the acidity level or the increasing soaking time causes an increase in the Si/Al Ratio. Table 1, natural zeolite modified NZD, indicates that the Si/Al ratio is the highest, while the total pore volume and surface area are the lowest. The excessive use of acid during the dealumination process can negatively affect zeolite's structure and properties, altering mesopores' size, number, and distribution [30].

Further insights into the porous structure of the catalysts are provided through the mesopore and micropore volumes. Generally, there is an increase in both mesopore and micropore volumes in the modified catalysts, contributing to a more intricate porous network that could facilitate enhanced mass transfer and adsorption processes. Simultaneously, the total pore volume, an aggregate of mesopores and micropores, exhibits a discernible rise in the modified catalysts, indicating an overall improvement in porosity. This enhancement, combined with the increased surface area, implies a potential boost in the catalyst's capability to

Table 1 Surface area, pore volume, and radius for both untreated and modified natural zeolite (NZ).

Parameter		Catalyst properties								
		NZ	NZA	NZB	NZC	NZD	Ni/NZA	Ni/NZB	Ni/NZC	Ni/NZD
Si/Al Ratio		5.08	10.73	24.93	22.79	27.05	7.12	5.76	8.44	9.95
Surface area	(m^2/g)	28.62	147.7	136.3	111.4	104.3	97.91	72.74	71.32	65.48
Mesopore volume	(cm^3/g)	0.08	0.11	0.09	0.07	0.006	0.07	0.06	0.06	0.05
Micropore volume	(cm^3/g)	0.01	0.07	0.06	0.05	0.005	0.06	0.06	0.05	0.04
Total pore volume	(cm^3/g)	0.09	0.181	0.157	0.123	0.118	0.132	0.119	0.107	0.092
Average pore radius	(nm)	0.635	2.452	2.304	2.318	2.293	2.437	2.292	2.314	2.265

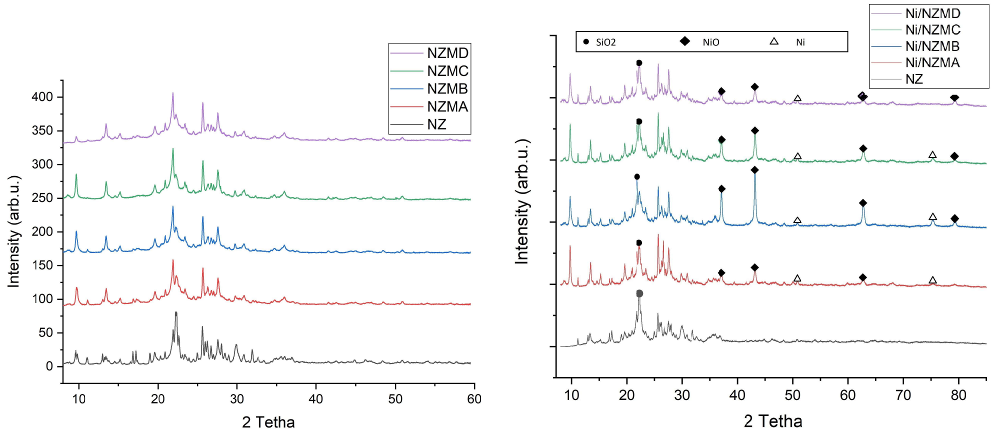

(a) (b)

Fig. 3 XRD pattern of (a) a natural zeolite catalyst subjected to modification and (b) a natural zeolite nickel modification to Ni impregnation.

accommodate reactants and facilitate catalytic reactions [29]. The average pore radius, a crucial parameter influencing diffusion and transport phenomena, experiences a notable increase in the modified catalysts, further emphasizing the impact of modification on the catalyst's structural characteristics [29].

The introduction of nickel into the modified NZ catalysts (Ni/NZA, Ni/NZB, Ni/NZC and Ni/NZD) is likely to have additional implications for catalytic activity. The observed decrease in the Si/Al ratio after nickel impregnation signifies a significant alteration in the catalyst properties. Before Ni impregnation, the XRD analysis of the zeolite catalysts as shown in Fig. 3 revealed a pronounced peak corresponding to SiO_2, indicating a relatively higher abundance of silicon dioxide compared to aluminum oxide. In zeolite synthesis, aluminum oxide typically contributes to the structure and framework of the zeolite. The specific type of aluminum oxide in zeolite is crucial for its catalytic properties. However, the SiO_2 peak being higher than the aluminum oxide peak in the initial XRD data indicates an imbalance in the Si/Al ratio, potentially impacting the catalytic performance. Upon nickel impregnation, there is a noteworthy shift in the XRD peaks. The Si/Al ratio decreases, suggesting a reduced abundance of aluminum in the catalyst structure. This alteration is accompanied by an adjustment in the peak heights of SiO_2 and aluminum oxide. Post-impregnation, the SiO_2 peak becomes comparable or even lower than the aluminum oxide peak, indicating a more balanced Si/Al ratio. This shift in peak heights implies a successful incorporation of nickel species into the zeolite structure, leading to modifications in the catalyst's composition and potentially enhancing its catalytic activity. The reduction in Si/Al ratio post-impregnation is likely attributed to the introduction of nickel species, which occupy specific sites within the zeolite framework, displacing silicon or aluminum atoms. This restructuring might result in a more uniform distribution of aluminum throughout the zeolite framework, impacting its catalytic behavior.

The Ni/NZA catalyst exhibits a substantial increase in surface area compared to the other Ni-loaded catalysts as shown in Table 1, potentially pointing towards synergistic effects between nickel and the modified NZA structure. The presence of nickel may contribute to the creation of additional active sites, thereby enhancing catalytic reactivity [29]. While the Si/Al ratio decreases compared to pre-Ni impregnation, it still remains elevated in the Ni-loaded catalysts, indicating

(a) Ni/NZMA

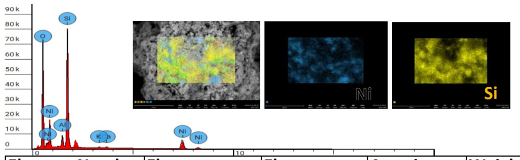

Element Number	Element symbol	Element Name	Atomic Conc.	Weight Conc.
28	Ni	Nickel	11,679	27,528

(b) Ni/NZMB

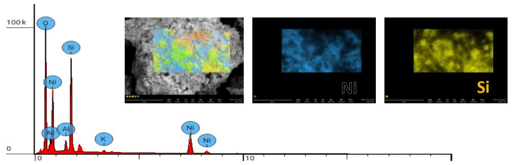

Element Number	Element Symbol	Element Name	Atomic Conc.	Weight Conc.
28	Ni	Nickel	22,463	45,954

(c) Ni/NZMC

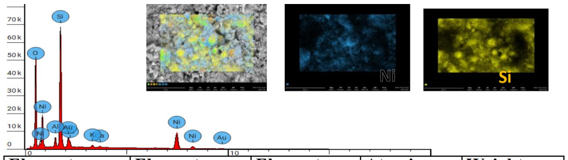

Element Number	Element Symbol	Element Name	Atomic Conc.	Weight Conc.
28	Ni	Nickel	15,869	32,265

(d) Ni/NZMD

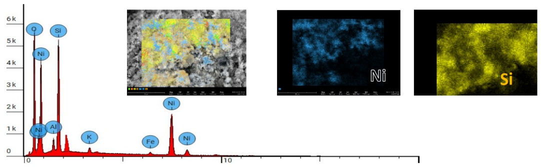

Element Number	Element Symbol	Element Name	Atomic Conc.	Weight Conc.
28	Ni	Nickel	10,046	23,159

Fig. 4 SEM images and EDS data of a natural zeolite catalyst that underwent modification and nickel impregnation.

the retention of acidity following modification [29]. Analyzing the pore characteristics of the Ni-loaded catalysts reveals interesting trends, with variations in mesopore and micropore volumes among the Ni-loaded catalysts. However, the total pore volume remains relatively consistent, indicating a balanced modification that maintains an overall porous structure. The average pore radius, although slightly varying, remains within a comparable range for the Ni-loaded catalysts. This consistency suggests that the introduction of nickel does not significantly alter the overall pore size distribution, which could be advantageous for maintaining effective diffusion and transport properties during catalytic reactions [29].

Referring to the additional information provided, zeolites with a low Si/Al ratio are stated to be more polar, indicating stronger absorption capacity, while those with high silicon content possess larger active centers suitable for catalytic applications [29]. Conversely, zeolites with high silica content exhibit a more homogenous surface and hydrophobic properties [31]. Aluminosilicates, forming a framework through aluminum and silicon atoms, introduce porosity, crucial for zeolite catalytic functionality. The acidity of zeolites, influenced by the Si/Al ratio, remains prominent even after modification and nickel loading. The discussion touches on the dual role of zeolite acidity, encompassing Bronsted and Lewis acid sites [32]. The increase in surface area and total volume observed in Table 1 is complemented by the insight that zeolite properties, such as surface homogeneity and hydrophobicity, may be influenced by the impregnation of Ni during modification [31].

The X-ray diffraction (XRD) patterns, (Fig. 3), provide insightful details about the structural characteristics of both the raw zeolite catalyst and the modified zeolite impregnated with nickel. The distinctive peaks associated with the support catalyst SiO_2 (JCPDS 39-1425) are evident at the broad peak around 22.3° [33], indicative of the amorphous structure of silica. This suggests that the modification process, including the introduction of nickel, does not alter the fundamental amorphous nature of the silica support. Additionally, peaks corresponding to the presence of nickel metal at angles 50.9° is discernible on the modified catalyst. The observation of these peaks aligns with the successful impregnation of nickel onto the zeolite structure.

Furthermore, the XRD analysis reveals the presence of NiO phase peaks (JCPDS 65-2901) at angles 37.2°and 43.2° on the nickel-impregnated catalyst. This indicates the formation of nickel oxide phases as a result of the modification process. The identification of these peaks provides valuable information about the crystalline structure and phase composition of the catalyst after nickel impregnation. During the reduction process of the catalyst, various possibilities arise. A fraction of Ni species may not undergo reduction completely, and the reduced Ni on the catalyst may undergo reoxidation back to NiO when exposed to air [34, 35]. These potential phenomena during the reduction process underscore the dynamic nature of the catalyst's behavior under different conditions.

Moreover, the nickel content determined through XRD testing corresponds with the SEM-EDS composition analysis shown in Fig. 4, reinforcing the consistency of the findings. The XRD analysis indicates an increase in nickel content in tandem with the heightened peak intensities in the XRD diffraction results. This observation is further supported by SEM-EDS testing, where the Ni/NZMB sample exhibits the highest nickel content. The correlation between XRD and SEM-EDS analyses reinforces the reliability of the analytical methods employed and provides a comprehensive understanding of the structural and compositional changes induced by the modification and nickel impregnation processes.

Thermogravimetric analysis of biomass across different catalysts

TGA data provides insights into the thermal behavior of various biomass samples at different temperatures. Initially, at 40 °C, all samples show minimal mass changes, indicating stability. As the temperature increases to 60–100 °C, a slight mass decrease is observed, suggesting the release of volatile components or moisture. The main decomposition phase occurs between 200–500 °C, with biomass + Ni/NZMB and biomass + Ni/NZMC exhibiting higher stability. In the range of 600–800 °C, substantial mass loss is seen, with biomass + NZMC consistently displaying the highest loss. Beyond 800 °C, a plateau is reached, indicating major decomposition completion. Although the Si/Al ratio decreases post-Ni impregnation, it remains high in Ni-loaded catalysts, maintaining acidity even after modification. The heat flow analysis at specific temperatures reveals varied thermal behavior influenced by different catalysts. The Si/Al ratio is known to be related to the proximity of the local structure of Al to Si, which can affect the increase in interaction between Brønsted acid sites and guest molecules. The relationship between Brønsted acid sites and the distribution of Al frameworks also increases [36]. The acid strength of the Brønsted acid sites is known to affect the catalyst's ability to break carbon chain bonds [37]. So, the role of zeolite here is not only as a support for nickel catalysts but also to create Brønsted acid sites that can affect the spatial interaction of hydrocarbon gases during the gasification process.

For instance, at 471.95 °C, biomass + NZMC exhibits significant heat flow, suggesting enhanced thermal interactions, possibly due to Ni/NZMC catalytic effects. The subsequent temperature points show unique heat flow patterns, emphasizing catalyst-specific thermal dynamics [38, 39].

The dataset explores the intricate relationships between temperature, relative mass change, and heat flow in diverse combinations of biomass and metals. Throughout the temperature range, a consistent decline in relative mass change is observed, indicating a general trend across all combinations. Notably, biomass + Ni/NZMC stands out with a pronounced negative mass change, suggesting heightened sensitivity to temperature fluctuations and potential reactions at elevated temperatures. The examination of heat flow data introduces a nuanced perspective. At 471.95 °C, biomass + NZMC displays a substantial heat flow of 167.22 mW, indicating distinct thermal behavior. The Differential Thermal Analysis (DTA) further characterizes this thermal behavior, identifying three thermal zones: initial drying, hemicellulose decomposition, and cellulose decomposition (Fig. 5). The significant heat flow at 471.95 °C aligns with specific exothermic processes, particularly cellulose decomposition within biomass + NZMC.

Further analysis at specific temperature points provides deeper insights into the thermal interactions between biomass and different catalysts. For instance, at 472.95 °C, biomass + NZMB exhibits notable heat flow, suggesting considerable impact on thermal behavior. Similarly, at 480.95 °C, biomass + Ni/NZMA shows substantial heat flow, emphasizing its unique catalytic effects. However, other combinations show minimal or no significant heat flow at these temperatures, indicating the specificity of catalyst influence. Therefore, the detailed TGA data underscores the importance of catalysts in shaping the thermal decomposition of biomass. The observed heat flow patterns at specific temperatures reveal varying degrees of catalytic influence, offering valuable insights into the dynamic processes involved.

Syngas composition and yield using raw and modified NZs

A comprehensive breakdown of syngas composition across various catalysts and non-catalytic conditions, offering insights into their respective efficiencies is provided (Fig. 7). Beginning with Ni/NZMC, this catalyst exhibits notable efficiency in syngas production, boasting a high hydrogen content of 59%, coupled with a balanced composition of 27% CO and 9% CO_2 Ni/NZMB, while displaying a slight variation, maintains a favorable equilibrium between hydrogen production and carbon-containing gases. Ni/NZMA showcases effective catalytic activity, emphasizing hydrogen production while minimizing methane formation. The natural zeolite catalyst (NZ) demonstrates moderate efficiency, while the non-catalyst condition results in less efficient conversion. Further highlights the impact of nickel impregnation on modified natural zeolite, showcasing increased syngas production and a favorable shift in hydrogen composition (Fig. 7). This aligns with the findings of Vizcaino et al [40], emphasizing the substantial role of nickel in enhancing hydrogen production. Contrary to conventional beliefs, the catalyst with the largest specific surface area does not necessarily translate into the highest catalytic performance, emphasizing the intricate interplay between catalyst characteristics and efficiency.

The discussion extends to the Si/Al ratio, traditionally assumed to have a linear relationship with gasification results. However, this study reveals a non-linear relationship, underlining the multifaceted nature of catalyst performance beyond surface area considerations. Challenging conventional notions, the nuanced relationship between specific surface area and

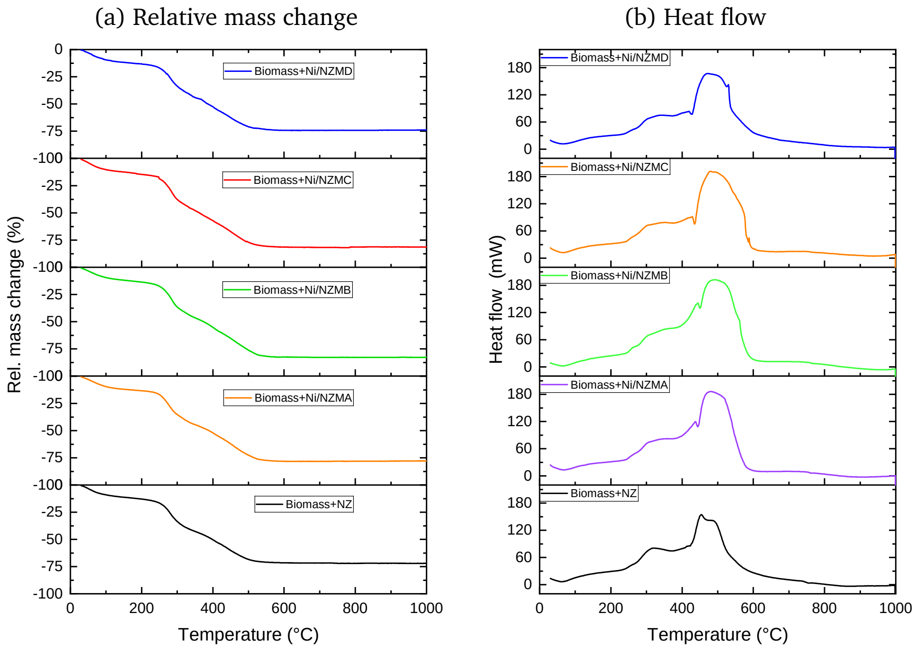
(a) Relative mass change (b) Heat flow

Fig. 5 Relative mass change and heat flow acquired through TGA testing.

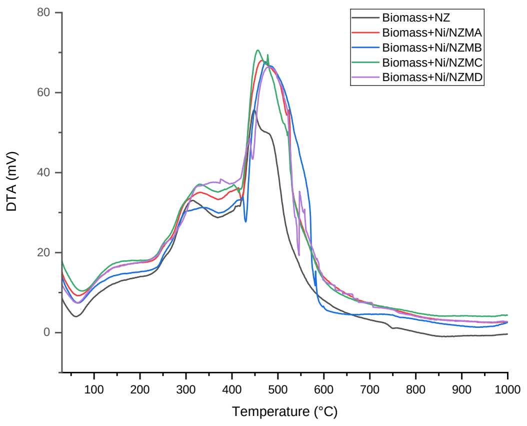

Fig. 6 DTA curves corresponding to biomass in the presence of different natural zeolite catalysts.

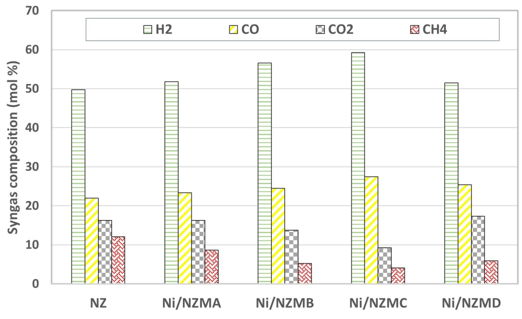

Fig. 7 Comparison between the syngas production from non-catalytic biomass gasification and the catalytic counterparts using natural zeolite (NZ) and modified zeolite impregnated with nickel (Ni/NZMA, Ni/NZMB, Ni/NZMC, Ni/NZMD).

catalytic performance becomes apparent, highlighting that a larger specific surface area is not the sole determinant of superior catalytic activity. Instead, the study suggests that the combination of an appropriate Si/Al ratio and BET surface area is crucial for stabilizing the reactivation process during gasification and steam reforming. This comprehensive understanding of the intricate interplay between nickel impregnation, Si/Al ratio, and specific surface area provides valuable insights for optimizing catalyst design in gasification and reforming processes. The findings underscore the necessity for a nuanced approach, considering multiple factors, to achieve superior catalytic performance in these complex reactions. This emphasizes the need for a holistic understanding of catalyst characteristics in designing efficient catalytic systems.

Moving to the gasification yield shown in Fig. 8, each catalyst's performance is elucidated. Starting with the non-catalyst condition, the gasification yield is 69%, with a breakdown of 11.40% tar and 19.60% char. This suggests effective conversion of biomass into gaseous products, with a notable portion of biomass transformed into gas. Moving to the NZ catalyst, the gasification yield increases to 77.70%, indicating enhanced efficiency in converting biomass into gas.

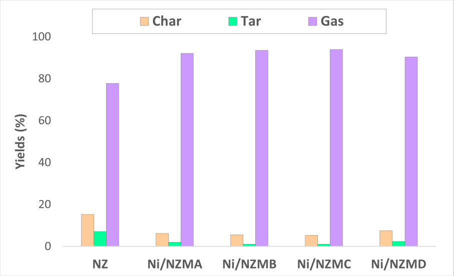

Fig. 8 Gas, tar, and char production during biomass gasification using pure biomass, natural zeolite catalyst, modified natural zeolite, and nickel-impregnated zeolite.

The tar and char percentages decrease to 7.06% and 15.24%, respectively, highlighting a cleaner gasification process with reduced by-products. Ni/NZMA, a modified zeolite catalyst impregnated with nickel, exhibits an impressive 92.04% gasification yield. This higher yield suggests a further improvement in biomass conversion, with only 1.90% tar and 6.06% char. The reduced tar and char percentages indicate a more efficient gasification process with a focus on producing gaseous products. Ni/NZMB, another nickel-impregnated zeolite catalyst, demonstrates a 93.52% gasification yield. The distribution reveals a highly effective conversion process, with only 0.96% tar and 5.52% char. This points towards superior efficiency in biomass conversion, emphasizing the catalyst's positive impact on the gasification process. Finally, Ni/NZMC, the third nickel-impregnated zeolite catalyst, achieves the highest gasification yield at 93.90%. The breakdown shows only 0.94% tar and 5.16% char, underlining its exceptional efficiency in transforming biomass into gaseous products. This catalyst's performance indicates a highly effective gasification process, with minimal production of tar and char by-products.

Therefore, the gasification yield results demonstrate the progressive improvement in biomass conversion efficiency with the introduction of zeolite catalysts, particularly those impregnated with nickel. The reduction in tar and char percentages across the nickel-impregnated catalysts highlights their positive impact on enhancing the gasification process, making them promising candidates for further exploration in biomass gasification applications.

The intricate interplay between temperature, catalysts, and biomass composition plays a pivotal role in shaping the thermal behavior and gasification efficiency of biomass. The thermal degradation of biomass is a complex process influenced by the specific interactions between the catalysts and the biomass constituents at varying temperatures [12, 41]. Understanding this interplay is crucial for optimizing gasification processes and enhancing the overall efficiency of biomass conversion. Temperature serves as a critical factor in influencing the kinetics of biomass decomposition. As the temperature increases, various thermal events unfold, including the release of volatile components, hemicellulose and cellulose decomposition, and ultimately the transformation of solid biomass into gaseous products. The TGA analysis highlights how different catalysts can either enhance or mitigate these thermal events at specific temperature ranges. For instance, biomass + Ni/NZMB and biomass + Ni/NZMC exhibit higher stability in the major decomposition phase, suggesting that the addition of nickel to the natural zeolite catalyst influences the thermal behavior of biomass, possibly by promoting more controlled decomposition reactions.

The catalytic effects on thermal behavior become particularly evident in the heat flow analysis at specific temperatures. The substantial heat flow observed, such as in the case of biomass + NZMC at 471.95 °C, indicates increased thermal activity associated with the catalytic effects of nickel impregnation. This heightened thermal activity could be linked to enhanced catalytic reactions, potentially involving the decomposition of cellulose or other biomass constituents. In contrast, the absence of significant heat flow in other combinations at the same temperature suggests variations in the catalytic influence, highlighting the specificity of catalyst-biomass interactions.

The syngas composition data further elucidate the catalytic effects on gasification efficiency. Notably, the varying efficiencies exhibited by different catalysts, such as Ni/NZMC's high hydrogen content, underscore the selective catalytic promotion of specific gasification reactions. The nuanced relationship between the Si/Al ratio and gasification results challenges conventional beliefs, emphasizing the importance of catalyst characteristics beyond surface area considerations. This includes the need for an appropriate Si/Al ratio and BET surface area, indicating that catalyst design intricacies contribute significantly to the overall gasification process. Moving to gasification yield analysis, the progressive improvement in biomass conversion efficiency with the introduction of zeolite catalysts, especially those impregnated with nickel, underscores their positive impact. The reduced tar and char percentages across nickel-impregnated catalysts further highlight their efficacy in enhancing the gasification process. For instance, Ni/NZMC achieving the highest gasification yield emphasizes its exceptional efficiency in transforming biomass into gaseous products. Therefore, the intricate interplay between temperature, catalysts, and biomass composition involves a delicate balance of catalytic reactions and thermal dynamics. Catalysts, particularly those impregnated with nickel, exert specific effects on biomass decomposition, influencing the efficiency of gasification processes. The temperature-dependent behaviors and gasification yield results collectively underscore the need for a nuanced approach in catalyst design, considering multiple factors to achieve superior catalytic performance in biomass conversion applications. This comprehensive understanding offers valuable insights for optimizing gasification processes and advancing the field of biomass utilization for energy production.

The superior gas yield and higher hydrogen content observed in the syngas produced by biomass + Ni/NZMA, biomass + Ni/NZMB, biomass + Ni/NZMC and biomass + Ni/NZMD combinations can be attributed to several potential mechanisms associated with the nickel impregnation in the natural zeolite catalysts. Firstly, nickel is known for its catalytic activity in reforming reactions, particularly steam reforming of hydrocarbons. In the gasification process, the presence of nickel can facilitate the reforming of tar and methane, leading to an increased production of hydrogen-rich syngas (Fig. 7). The catalysts, especially Ni/NZMC, may actively participate in breaking down complex hydrocarbons into simpler gaseous components, thus enhancing the overall gas yield and hydrogen content.

Secondly, nickel acts as a promoter for water-gas shift reactions, which play a crucial role in adjusting the composition of syngas. These reactions involve the conversion of carbon monoxide (CO) and water vapor (H_2O) into carbon dioxide (CO_2) and hydrogen (H_2). The promotion of water-gas shift reactions by nickel can contribute to an elevated hydrogen content in the syngas, as observed in Fig. 6. Furthermore, nickel is capable of catalyzing the decomposition of hydrocarbons and biomass constituents at lower temperatures. This catalytic activity promotes the release of volatile components during the initial stages of gasification, ensuring efficient conversion of biomass into gaseous products. The presence of nickel in the zeolite catalysts, particularly in Ni/NZMA, Ni/NZMB, Ni/NZMC and Ni/NZMD, enhances the gasification efficiency by accelerating these decomposition reactions.

Moreover, the specific characteristics of each nickel-impregnated zeolite catalyst may contribute to the observed variations in gas yield and syngas composition. For example, the unique structure or surface properties of Ni/NZMB may favor specific reactions leading to a higher gas yield at certain temperature ranges. Overall, the catalytic effects of nickel impregnation in the natural zeolite catalysts likely involve a combination of reforming reactions, water-gas shift reactions, and enhanced decomposition of biomass constituents. The synergy of these mechanisms contributes to the increased gas yield and higher hydrogen content in the syngas, making these catalysts promising candidates for improving the efficiency of biomass gasification processes. Further detailed investigations and kinetic studies would be essential to unravel the specific pathways and interactions underlying the catalytic effects of nickel in these zeolite catalysts.

CONCLUSION

The study explored biomass's thermal behavior and gasification efficiency using various NZ catalysts, including those modified with nickel. The results provided insights into how catalyst properties, temperature, and biomass composition interact. The analysis of zeolite catalysts (NZA, NZB, NZC, NZD) showed changes in their Si/Al ratio, surface area, and pore structure, indicating successful modifications. Nickel impregnation also altered the catalysts' structure, as seen in changes to X-ray diffraction patterns and Si/Al ratios. TGA revealed that biomass behaved differently depending on the catalyst, with nickel-impregnated zeolites showing specific effects on biomass decomposition at different temperatures. At 471.95 °C, biomass with Ni/NZMC showed stronger thermal interactions, likely linked to cellulose breakdown. Nickel-impregnated catalysts improved syngas composition, increasing hydrogen content and reducing tar and char compared to non-catalytic and natural zeolite setups. These findings highlight the importance of factors like Si/Al ratio and surface area in achieving better catalytic performance.

Acknowledgements: The authors express our sincere gratitude to the Rector of Universitas Sebelas Maret for their generous support in the form of funding grants (PKPTDN, Mandatory, PUT, and PTUPT) provided from 2021 to 2024.

REFERENCES

1. Derbe T, Temesgen S, Bitew M (2021) A short review on synthesis, characterization, and applications of zeolites. *Adv Mater Sci Eng* **2021**, 6637898.
2. Rahman ROA, El-Kamash AM, Hung Y-T (2022) Applications of nano-zeolite in wastewater treatment: An overview. *Water* **14**, 137.
3. Kraljević Pavelić S, Simović Medica J, Gumbarević D, Filošević A, Pržulj N, Pavelić K (2018) Critical review on zeolite clinoptilolite safety and medical applications *in vivo*. *Front Pharmacol* **9**, 1350.
4. Nakhli SAA, Delkash M, Bakhshayesh BE, Kazemian H (2017) Application of zeolites for sustainable agriculture: A review on water and nutrient retention. *Water Air Soil Pollut* **228**, 464.
5. Somphon W, Loisruangsin A (2023) ZIF-8, chitosan and β-cyclodextrin-incorporated ZIF-8 nanohybrid for improving drug delivery. *ScienceAsia* **49**, 776–785.
6. Younas F, Bibi I, Zulfqar A, Shahid M, Shakoor MB, Hussain MM, Niazi NK, Nawaz MF (2023) Environmental applications of natural and surface-modified zeolite. In: Vithanage M, Lazzara G, Rajapaksha AU (eds) *Clay Composites: Environmental Applications*, Springer Nature, Singapore, pp 373–396.
7. Liu Z, Zhu J, Wakihara T, Okubo T (2019) Ultrafast synthesis of zeolites: breakthrough, progress and perspective. *Inorg Chem Front* **6**, 14–31.
8. Salahudeen N (2022) A review on zeolite: Application, synthesis and effect of synthesis parameters on product properties. *Chem Africa* **5**, 1889–1906.

9. Heryanto R, Rohaeti E, Wulansari L, Arif Z, Tri W, Riza B (2022) Potentiometric sensor for chromium (VI) using a composite of diphenylcarbazide-natural zeolite-modified membrane electrodes. *ScienceAsia* **48**, 434–442.
10. Kumar J, Vyas S (2024) Comprehensive review of biomass utilization and gasification for sustainable energy production. *Environ Dev Sustain*. **27**, 1–40.
11. Sharma VK, Braccio G, Anyanwu CN (2024) Innovative power generation technologies for improved household energy delivery and sustainable future: Classical solutions from ENEA Research Centre, Trisaia Italy. *Processes* **12**, 389.
12. Narnaware SL, Panwar NL (2021) Catalysts and their role in biomass gasification and tar abetment: A review. *Biomass Convers Biorefinery*.
13. Magyarová Z, Králik M, Soták T (2023) Utilization of zeolite catalysts in biomass exploitation: A minireview. *Monatsh Chem* **154**, 815–835.
14. van der Graaff WNP, Pidko EA, Hensen EJM (2016) Zeolite catalysis for biomass conversion. In: Xiao F-S, Meng X (eds) *Zeolites in Sustainable Chemistry: Synthesis, Characterization and Catalytic Applications*, Springer, Berlin, Heidelberg, pp 347–372.
15. Waluyo J, Richards T, Makertihartha I, Susanto H (2017) Modification of natural zeolite as a catalystfor steam reforming of toluene. *Asean J Chem Eng* **17**, 37–45.
16. Prihadiyono FI, Lestari WW, Putra R, Aqna ANL, Cahyani IS, Kadja GTM (2022) Heterogeneous catalyst based on nickel modified into Indonesian natural zeolite in green diesel production from crude palm oil. *Int J Technol* **13**, 931–943.
17. Cai T, Tursun R, Wu Z, Sun Q (2023) Synthesis and gas sensing properties of amorphous $NiTiO_3$. *ScienceAsia* **49**, 523–528.
18. Liu D, Slocombe M, AlKinany H, AlMegren J, Wang J, Arden A, Vai S, Gonzalez-Cortes T, et al (2016) Advances in the study of coke formation over zeolite catalysts in the methanol-to-hydrocarbon process. *Appl Petrochemical Res* **6**, 209–215.
19. Alaba PA, Sani YM, Mohammed IY, Wan Daud WMA (2016) Insight into catalyst deactivation mechanism and suppression techniques in thermocatalytic deoxygenation of bio-oil over zeolites. **32**, 71–91.
20. Muhammad I, Makwashi N, Ahmed TG, Manos G, Zhao D (2023) A mechanistic model on catalyst deactivation by coke formation in a CSTR reactor. *Processes* **11**, 944.
21. Bingre R, Li R, Wang Q, Nguyen P, Onfroy T, Louis B (2019) Porosity design of shaped zeolites for improved catalyst lifetime in the methanol-to-hydrocarbons reaction. *Catalysts* **9**, 545.
22. Zang J, Yu H, Liu G, Hong M, Liu J, Chen T (2023) Research progress on modifications of zeolite Y for improved catalytic properties. *Inorganics* **11**, 22.
23. Han X, Zhou X, Ji T, Zeng F, Deng W, Tang Z, Chen R (2024) Boosting the catalytic performance of metal-zeolite catalysts in the hydrocracking of polyolefin wastes by optimizing the nanoscale proximity. *EES Catal* **2**, 300–310.
24. Al-Samhan M, Al-Fadhli J, Al-Otaibi AM, Bouresli R (2023) Synthesis of micromesoporous zeolite-alumina catalysts for olefin production from heavy crude oil. *Int J Chem Eng* **2023**, 7302409.
25. Wei P, Zhang X, Liu W, Huang X, Fa, Y, Yan R, Zhang L, Wang Y, et al (2020) Synthesis of Ni-modified ZSM-5 zeolites and their catalytic performance in *n*-octane hydroconversion. *Front Chem* **8**, 586445.
26. Bacariza MC, Graça I, Westermann A, Ribeiro MF, Lopes JM, Henriques C (2016) CO_2 hydrogenation over Ni-based zeolites: Effect of catalysts preparation and pre-reduction conditions on methanation performance. *Top Catal* **59**, 314–325.
27. Hamidzadeh M, Ghassemzadeh M, Tarlani A, Sahebdelfar S (2018) The effect of hydrothermal impregnation of Ni, Co, and Cu on HZSM-5 in the nitrogen oxide removal. *Int J Environ Sci Technol* **15**, 93–104.
28. Peron DV, Zholobenko VL, de la Rocha MR, Oberson de Souza M, Feris LA, Marcilio NR, Ordomsky VV, Khodakov AY (2019) Nickel-zeolite composite catalysts with metal nanoparticles selectively encapsulated in the zeolite micropores. *J Mater Sci* **54**, 5399–411.
29. Ward JW (1967) The nature of active sites on zeolites: I. The decationated Y zeolite. *J Catal* **9**, 225–236.
30. Schwieger AG, Machoke T, Weissenber, Alexandra A, Inayat T, Selvam M, Klumpp A, Inayat W (2016) Hierarchy concepts: Classification and preparation strategies for zeolite containing materials with hierarchical porosity. *Chem Soc Rev* **45**, 3353–3376.
31. Corma A (2003) State of the art and future challenges of zeolites as catalysts. *J Catal* **216**, 298–312.
32. Alberti A (1997) Location of Bronsted sites in mordenite. *Zeolites* **19**, 411–415.
33. Barrai F, Jackson T, Whitmore N, Castaldi MJ (2007) The role of carbon deposition on precious metal catalyst activity during dry reforming of biogas. *Catal Today* **129**, 391–396.
34. Nitta Y, Imanaka T, Teranishi S (1985) Preparation chemistry of precipitated Ni/SiO_2 catalysts for enantioselective hydrogenation. *J Catalysis* **96**, 429–438.
35. Blackmond DG, Ko EI (1984) Preparation and characterization of well-defined Ni/SiO_2 catalysts. *ApplCatalysis* **13**, 49–68.
36. Yi F, Xu D, Tao Z, Hu C, Bai Y, Zhao G, Chen H, Cao J-P, et al (2022) Correlation of Brønsted acid sites and Al distribution in ZSM-5 zeolites and their effects on butenes conversion. *Fuel* **320**, 123729.
37. Handoko DSP, Triyono T (2023) The effect of acid strength of Bronsted acid site on the ability of catalyst to break the carbon chain bonds of 1-octadekenes into alkanes and short chain alkenes as a sub-stitute for fossil fuel. **46**, 1311.
38. Lu X, Wang Y, Estel L, Kumar N, Grénman H, Leveneur S (2020) Evolution of specific heat capacity with temperature for typical supports used for heterogeneous catalysts. *Processes* **8**, 911.
39. Farpón MG, Peláez R, Recio V, Atakan B, Zaldo C, Prieto G (2023) Multifunctional materials for catalyst-specific heating and thermometry in tandem catalysis. *J Mater Chem A* **11**, 19854–19859.
40. Vizcaino AJ, Carrero A, Calles JA (2007) Hydrogen production by ethanol steam reforming over Cu-Ni supported catalysts. *Int J Hydrog Energ* **32**, 1450–1461.
41. Lin L, Han X, Han B, Yang S (2021) Emerging heterogeneous catalysts for biomass conversion: studies of the reaction mechanism. *Chem Soc Rev* **50**, 11270–11292.